J. of Thermal Science Vol.6, No.3

JTS

Flow Visualization and Topological Analysis of a Turbine Rotor Cascade with Tip Clearance

Han Wanjin Liu Fengjun Zhong Jingjun Wang Zhongqi

Department of Power Engineering, Harbin Institute of Technology, Harbin, 150001, China

By means of ink trace visualization and topological analysis, this paper investigates the topological structure of the flow pattern surrounding both endwalls and blade surfaces for a low aspect ratio linear rotor cascade with tip clearance. The structure of the flow pattern shows that most of the singular points and separation lines are located in the upper half span region of the tested cascade where the aerodynamic behaviors are deteriorated.

Keywords: turbine rotor cascade, tip clearance, flow visualization, topological analysis.

INTRODUCTION

Recently significant attention has been given to the fine structure within the flow field of turbomachinery. In general, the study of this problem contains two aspects. The first is to visualize the solid surface flow and topologically analyze the singular points to investigate their numbers, types and locations and the skin friction line patterns in the flow field nearest to the wall. This aspect aims at obtaining a certain amount of wall flow information. The second aspect, on the other hand, carries out detailed flow field measurements and visualizations to acquire centralized vortex structures, and their interactions with the mainstream. However, only if the two aspects should be employed simultaneously, all the features of the flow field would be outlined. Just as Dallmann[1] pointed out that surface flow pattern alone cannot provide a unique interpretation of the flow field and studying the three-dimensional structure of the flow field requires the examination of the surface skin–friction lines and the internal flow field itself.

Sears[2] firstly applied the topological analysis to the fluid mechanics by studying the features of limiting streamlines. Legendre et al[3] went further into the continuous postulate of the vector fields constructed by the limiting streamlines, and studied the natures of singular points of finite number in the vector fields. Lighthill[4] considered that studying the surface flows is more suitable with the skin–friction lines than the limiting streamlines. He integrated the topological invariant of a curved surface (Euler characteristic) with the total number of nodes and saddles in a shear stress vector field on the closed surface. According to his viewpoints, for an isolated three-dimensional body immersed in non-boundary flow field, the topological rule is supported by the well-known Poincare-Bendixon (PB) theorem that the sum of nodes minus the sum of the saddles is two. Hunt et al[5] extended the PB theorem to analyze the patterns of section velocity vector fields. Kang Shun[6,7] firstly applied the topology to study the flow fields in turbomachinery, and developed topological rules for analyzing the flow patterns on endwalls and sections of the cascades without tip clearance. However, up to now the topological structures on the surface and section in turbine rotor cascades with tip clearance have seldom appeared as yet. This paper concentrates on the research of this problem. The measurement results and secondary flow structure will be described in other paper.

TEST FACILITY

The test facility is shown in Fig.1. This paper adopts the same tested blade profile as that

Received October, 1996.

of Yamamoto[8], but enlarged by 1.7287. Table 1 presents the enlarged profile coordinates. The other principal geometrical and aerodynamic parameters of the cascade are:

Blade chord $c = 121.49$ mm
Axial chord $B = 120$ mm
Pitch $s = 90$ mm
Aspect ratio $h/c = 0.905$
Pitch-chord ratio $s/c = 0.74$
Maximal thickness of profile -chord ratio
Maxthick/c = 0.257
Radius of blade leading edge $R_1 = 6.75$ mm
Radius of blade trailing edge $R_2 = 3.37$ mm
Number of blades $N_b = 6$
Cascade inlet angle (measured from axial direction)
$\alpha_1 = 50°$
Cascade exit angle $\alpha_2 = 57°$
Cascade turning angle $\Delta\beta = 107°$
Relative clearance $\tau/h = 0.023$
Inlet total pressure $p_0^* = 10730.4$ Pa
Mach number at the midspan of exit plane
$M = 0.3$
Reynolds number at the midspan of exit plane
(on the basis of blade chord) $Re = 8.3 \times 10^5$
Thickness of inlet endwall boundary layer
$\delta = 24$ mm

Ink trace visualizations were performed on both endwalls and blade surfaces.

Table 1 Blade profile coordinates

No	X	Y_P	Y_S
1	0.00000	0.000000	-10.94124
2	7.05885	0.54743	-21.17658
3	14.11772	-3.45883	-30.00015
4	21.17658	-7.97652	-37.05901
5	28.23543	-11.29417	-42.35315
6	35.29430	-13.76477	-45.52964
7	42.35315	-14.96479	-47.64730
8	49.41200	-14.96479	-48.00024
9	56.47087	-13.97654	-47.29435
10	63.52973	-11.85888	-45.17671
11	70.58860	-8.47063	-41.85904
12	77.64745	-4.58826	-36.70606
13	84.70630	0.91765	-31.41191
14	91.76517	7.41180	-22.58835
15	98.82402	15.03537	-12.70595
16	105.88288	22.94128	-0.70588
17	112.94174	31.41191	12.35230
18	120.00060		26.11777

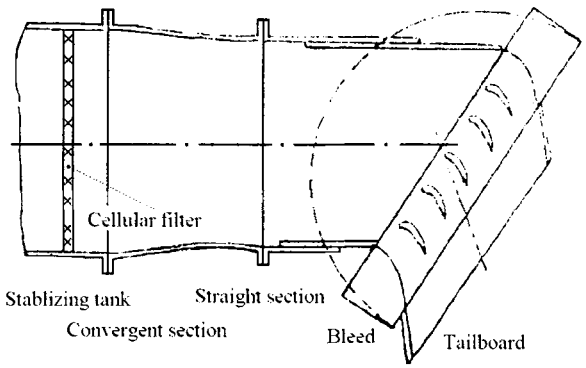

Fig.1 Experimental equipment

EXPERIMENTAL RESULTS AND DISCUSSION

The Topological Rules

The Poincare theorem, suitable to analyze the pattern on a curved surface, can be described as follows: if a tangential vector field is shown on the curved surface Q and continuous except at limited number of singular points, the sum of nodes minus the sum of saddles ($\sum N - \sum S$) on the curved surface is equal to the Euler characteristic $X(Q)$ of the surface:

$$\sum N - \sum S = X(Q) \tag{1}$$

The surface of a linear cascade with tip clearance can be divided into two disconnected surfaces as the upper endwall surface on the tip clearance side (from here on we define it as endwall with clearance) and the union of the low endwall with blade surfaces, each surface having a number of singular points.

We now examine the topological rule for the union of the lower endwall with blade surfaces. Stretch the endwall upstream and downstream far enough so that the flow is uniform, and bend the endwall to connect its front and back edges, forming a cylinder. Then extend both ends of the cylinder to an infinite distance, and bend it and connect its ends to form a torus. As a result, the lower endwall and blade surface are topological equivalent to the torus. The Euler characteristic of the torus is zero. According to formula (1), the number of the singular points in the skin-friction field on the lower endwall and blade surface in a pitch should obey the following formula:

$$\sum N_{bh} - \sum S_{bh} = 0 \tag{2}$$

where $\sum N_{bh}$ and $\sum S_{bh}$ denote the numbers of total node points and saddle points on these surfaces respectively.

Similarly, the endwall with clearance is also topologically equivalent to a torus. Let $\sum N_c$ and $\sum S_c$ represent the total numbers of nodes and saddles on the endwall surface, respectively, we get:

$$\sum N_c - \sum S_c = 0 \tag{3}$$

Then the topological rule for the cascade with tip clearance can be obtained by adding Eq.(2)and (3), as follows:

$$(\sum N_{bh} + \sum N_c) - (\sum S_{bh} + \sum S_c) = 0 \tag{4}$$

or

$$\sum N - \sum S = 0 \tag{5}$$

where $\sum N = \sum N_{bh} + \sum N_c$, $\sum S = \sum S_{bh} + \sum S_c$, that is to say, the total numbers of the nodes and saddles in the flow pattern surrounding the solid surface of a cascade with tip clearance would be equal to each other in a whole cascade or in a pitch.

The transverse section (the section whose normal is the cascade axis) of the cascade with tip clearance can be topologically transformed into an annular plane (Fig.2). This annular plane can then be topologically deformed into a half torus, i.e., the surface A in Fig.2(c). In the domain of the half torus, corresponding to the transverse section of cascade passage, there exist nodes and saddles, and on the boundary of the domain there exist half nodes and half saddles.

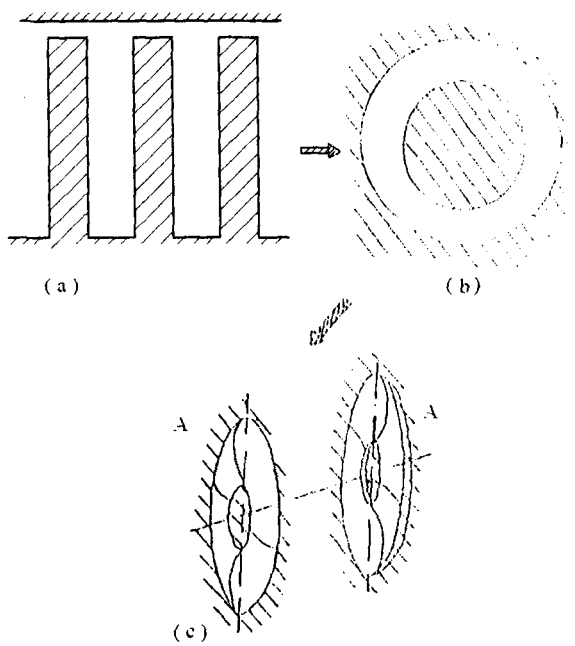

Fig.2 Topological equivalent graphs of the traverse section of an rectangular cascade

Suppose there exists a mapping of half torus A' (Fig.2(c)) which corresponds to the half torus A in the meaning that the position, number and nature of the singular points on the half torus A' correspond to those on A, respectively. Connecting the two half torus, outer circular to outer circular and inner circular to inner circular, a complete torus is formed. Skin-friction lines surround the torus with a number of complete singular points, some of which being made up by pairs of the half points. So the topological rule can be obtained to analyze the flow pattern on the torus surface:

$$(\sum N_A + \sum N_{A'} + \sum N') - (\sum S_A + \sum S_{A'} + \sum S') = 0$$

where the subscripts A and A' denote the singular points on the half torus A and A', and N' and S' the numbers of the nodes and saddles comprising of pairs of the half singular points on the boundary respectively.

In summary, the topological rule controlling the number of singular points in cascade cross flow (or secondary flow) field with the existence of tip leakage flow is:

$$(\sum N + 0.5\sum N') - (\sum S + 0.5\sum S') = 0 \tag{6}$$

Endwall Flow Pattern with Tip Clearance

Fig.3 shows the ink trace visualization of the flow on the endwall with tip clearance of a linear turbine cascade. The lower energy fluids on this wall move in different directions under their moment of inertia and the different pitchwise pressure gradients in different regions. On the region of the endwall directly over the blade tip, the boundary layer flows from the pressure side to the suction side of the same blade, resulting

Fig.3 Ink trace visualization on endwall with a tip clearance

in non-orthogonal intersection of limiting streamline with the pressure side and near orthogonal intersection with the suction side. For the region of the endwall directly over the flow passage, the low energy fluid crosses over the passage from the adjacent blade pressure side to the blade suction side. As a result, a separation line (L_s) of the leakage vortex and a reattachment line (L_r) are generated. The limiting streamlines around the former converge to it, which implies the flow goes into flow field; the limiting streamlines around the latter diverge from the latter showing the flow goes towards the endwall.

Fig.4 presents a topological flow pattern on the endwall with tip clearance. Clearly a skin-friction line near the blade leading edge is split into two legs at the point denoted as saddle point S_h, which is the point where the inlet endwall boundary layer separates, generating a leading edge horseshoe vortex. Its suction side leg turns around the leading edge and joins with the tip leakage vortex separation line at about 25% axial chord downstream. The pressure side leg first extends a short distance downstream, then changes its direction at approximately 5% axial chord towards the suction side of the same blade, finally cross over the tip clearance and usually joins with the suction side leg. Sjolander et al[9] showed whether the inlet edge horseshoe vortex will be generated depends on the relative clearance (τ/h). When $\tau/h \leq 0.01$, the pressure side leg of the horseshoe vortex always stretches downstream, similar to the case of zero clearance. When τ/h increases to 0.033, the saddle point S_h disappeared and the leading edge horseshoe vertex is not visible. In addition, Fig.4 shows in the region enclosed by the separation lines of the saddle point S_h, the limiting streamlines are bound to converge towards the separation lines, forming the attachment node N_h very near downstream of the saddle point.

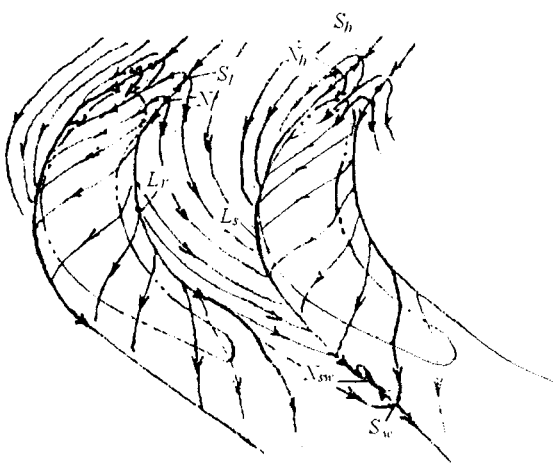

Fig.4 Topological analysis of flow pattern on endwall with tip clearance

The reattachment line (L_r) is comprised of the pitchwise highest pressure points. On the left side of L_r (in Fig.4) the limiting streamlines from L_r pass over the tip clearance to converge towards the leakage vortex separation line L_s near the suction side of the same blade. On the right side of L_r, the limiting streamlines cross over the passage to merge with the leakage vortex separation line L_s near the adjacent blade suction side. This phenomenon results from the reattachment line (L_r) stretching downstream in a way of keeping itself close to the blade pressure side. In addition, as shown in Fig.4, an attachment node N_L and a saddle point S_L are topologically formed near the upstream region (blade leading edge) of the reattachment line. Even though it is hard to identify the origin of the leakage vortex separation from Fig.3, the origin is likely to be the saddle point S_L. The rolling-up of the tip leakage vortex seems to start just downstream the leading edge near the suction side corner.

When the separation line (L_s) and reattachment line (L_r) extend downstream, these two lines will interact at approximate 1/3 axial chord downstream of the cascade, creating the saddle point S_w there. One branch of the separation line starting from the saddle point S_w further extends downstream, and the other branch stretches upstream and enters into the separation spiral node N_{sw}.

Apparently there are 3 saddle points, 2 attachment nodes and 1 spiral node in the endwall flow field with tip clearance. Moreover, the total number of saddle points and nodes satisfies Eq.(3), the topological rule.

Lower Endwall and Blade Surface Flow Pattern

Fig.5 and Fig.6 are flow pattern visualization on the lower endwall and blade surfaces. Fig.7 and Fig.8 are the topological analysis of the flow pattern corresponding to Fig.5 and Fig.6, respectively. The most complicated flow pattern is formed in the blade suction corner of the upper half span. Also, a reattachment line due to the half attachment node N'_{im} at the midspan of the leading edge is visible by comparing Fig.5,6 and Fig.7,8. It stretches spanwisely, crosses over the blade tip due to the leakage flow, reaches the suction edge at approximate 25% axial chord and extends downstream along the edge. Consequently, a saddle point S_c is created at about 60% axial chord. The separation line starting from the saddle point S_c is of two branches. One branch remains downstream till entering into the half separation node N'_t at the exit edge. The other extends downwards and downstream till ending at the half separation node N'_u lo-

cated at 60% blade span of the exit edge. The reattachment line downstream of S_c, slightly lower than the tip, goes upstream towards S_c on the suction surface. Because there is still a favorite profile pressure gradient, the length of the upstream going reattachment line is short and another attachment node N_c is topologically generated near the saddle point S_c. The reattachment line starting from the node N_c extends downwards and downstream along the suction surface until it reaches the half saddle point S'_u at 85% blade span of exit edge. The separation line on the blade tip suction edge starting from S_c is considered to be a convergent line between the blade tip limiting streamlines and upper suction surface limiting streamlines. It is associated with the secondary vortex, which rotates opposite to the tip leakage vortex. The presence and rotation of the vortex can be evidenced from the secondary flow vectors in the suction side upper corner (this will be described in another paper). Clearly, the convergent line of the limiting streamlines, which starts from S_c and is located below the reattachment line on upper half span suction surface, is the separation line of the upper passage vortex.

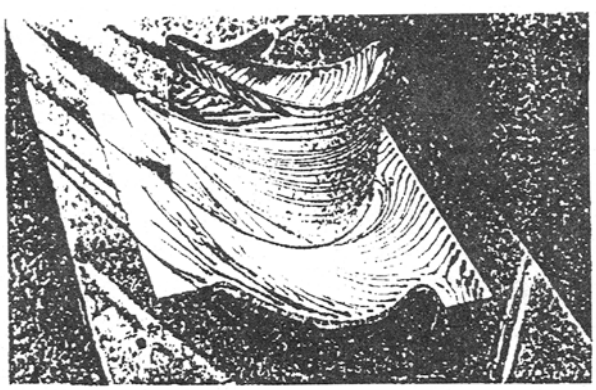

Fig.5 Ink trace visualization on blade tip, blade suction surface and lower endwall

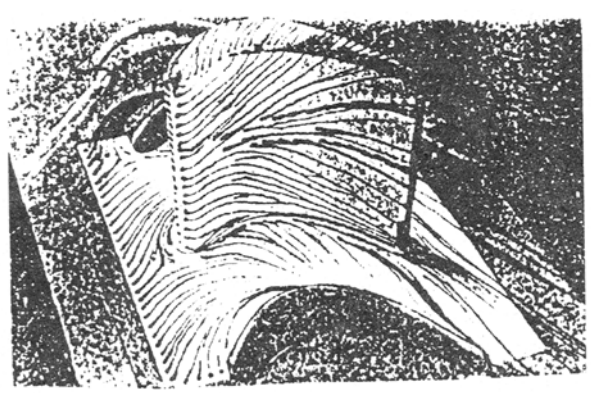

Fig.6 Ink trace visualization on blade tip, blade pressure surface and lower endwall

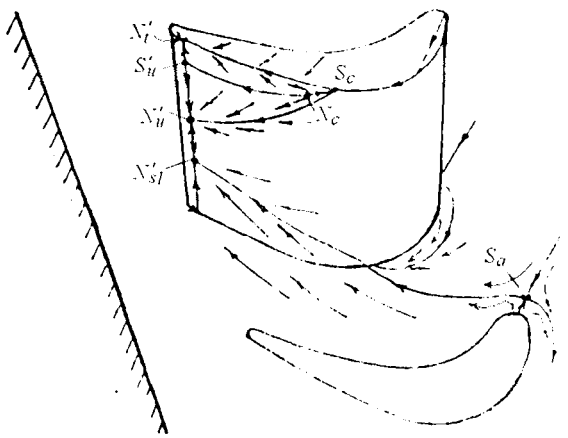

Fig.7 Topological analysis of flow on blade tip, blade suction surface and lower endwall

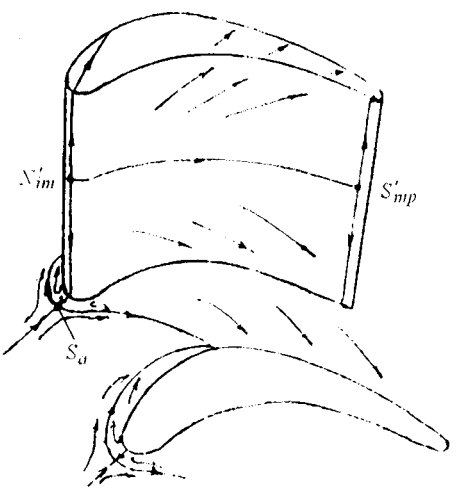

Fig.8 Topological analysis of flow on blade tip, blade pressure surface and lower endwall

The flow on the lower endwall and the suction surface of lower half span are analogous to these of a linear cascade without tip clearance. The inlet endwall boundary layer is separated at the saddle point in front of the leading edge of the cascade, generating the pressure and suction side legs of the horseshoe vortex. The separation line of the pressure side leg crosses over the passage, and is merged with one of the suction side leg of the adjacent blade at 45% axial chord where the separation line of the passage vortex is formed. The separation line of the passage vortex on the suction surface stretches upwards up to 34% blade span at the exit edge, finally ends at the half node N'_{SL}.

A reattachment line formed at midspan of pressure surface starts from the half attachment node N'_{im} at the leading edge, then stretches downstream and eventually ends at the half saddle point S'_{mp} lied on the exit edge. This is due to the face that the limiting streamlines on both blade tip and lower endwall converges

from the pressure side to the suction side, resulting in the streamlines on the pressure surface departing from midspan and converging towards both endwalls.

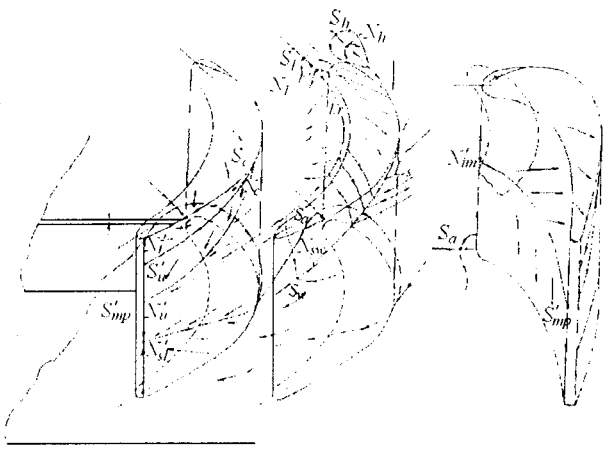

Fig.9 Topological analysis of flow pattern on the wall surfaces of whole cascade

There are 2 saddle points, 2 half saddle points, 1 attachment node and 4 half separation nodes, which satisfies Eq.(2) of the topological rule for the pattern of skin-friction lines on the lower endwall and blade surface.

Fig.9 is the topological analysis of the flow pattern on the wall surfaces of the whole turbine rotor cascade with a tip clearance. From this figure it can be seen that there are 5 saddle points, 3 attachment nodes, 1 spiral separation node, 2 half saddle points and 4 half nodes, which satisfies Eq.(4) or Eq.(5) of the topological rule for the turbine rotor cascade with tip clearances.

Topological Analysis of the Section Streamline Pattern

Fig.10 and Fig.11 show the topological analyses of the section flow located at the mid axial chord and the near exit, respectively. The topological structures in both positions agree with the velocity vectors. The difference between the two sections depends on the development of the tip leakage vortex, passage vortex and secondary vortex. The centralized vortices in the position of the mid chord section are characterized by the two clockwise rotation nodes near both endwalls. The node N_L near the lower endwall suggests the existence of the lower passage vortex. The reattachment line issued from N_L enters into the saddle point S_{ms} near the suction surface at the mid span. One branch of the separation line originating from S_{ms} goes into the half separation node N'_{sm} on the suction surface at the midspan, and the other branch goes into another saddle point S_{mp} near the pressure surface at the mid span. Meanwhile one branch of the half saddle point S_{mp} enters into the half saddle point S'_{up} on the upper endwall, the other branch surrounds around the lower passage vortex. The surface flows in the lower half span region in this section usually rotates clockwise due to the lower passage vortex.

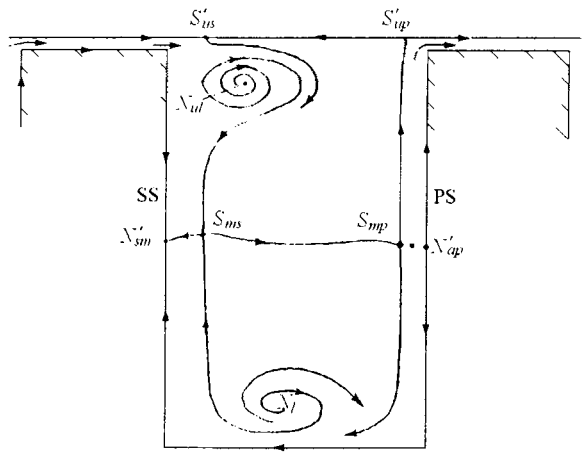

Fig.10 Topological analysis of section flow pattern located at mid axial chord

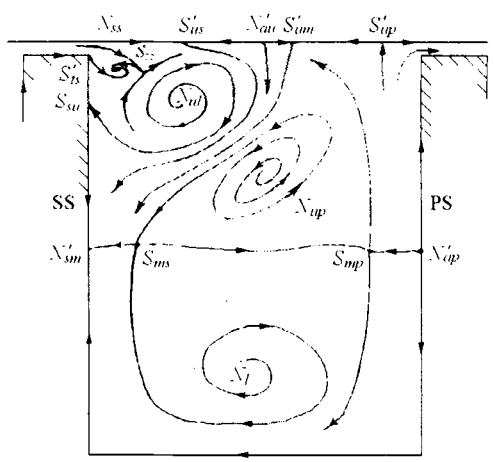

Fig.11 Topological analysis of section flow pattern located at axial chord

The separation lines issued from the saddle points S_h and S_L all converge to separation line L_s near the suction surface on the upper endwall, thus forming merely the leakage vortex N_{uL} in the first half passage of the upper half span. The reattachment line issued from the N_{uL} also enters into the saddle point S_{ms}. Evidently, on the upper endwall, there is the half saddle point S'_{us} near the suction side, and the half saddle point S'_{up} near the pressure side.

In the mid axial chord section there are 2 saddle points, 2 half saddle points, 2 nodes and 2 half nodes.

In this section, the total number of these singular points satisfies the topological rule Eq.(6).

In the transverse section close to the exit, the upper passage vortex and the tip leakage vortex further increase in intensity and scale and depart from the upper endwall and the blade surfaces. Besides, the flow in the upper half span experiences significant changes. Since the section is located behind the saddle point S_c, the upper passage vortex and the secondary vortex rotating counterclockwise are generated. There exist a small scale vortex near the blade tip suction edge, which may be a secondary vortex. A saddle point S_{ts} is formed between the secondary vortex and the tip leakage vortex. These vortices contribute to the creation of the upper passage vortex. Once the upper passage vortex is created, it rapidly develops towards the middle of the passage, but with less intensity and lower scale than those of the lower passage vortex . The vorticity of the three centralized vortices are originated from the upper endwall, blade surface and the tip clearance, therefore creating six different types of half singular points on these surfaces.

In the section close to the exit, there are 3 saddle points, 5 half saddle points, 4 nodes and 3 half nodes. The total number of the singular points satisfies the topological rule Eq.(6).

CONCLUSIONS

1. Due to the interaction between the leakage flow and the upper endwall crosswise flow of the rotor cascade with tip clearance, three among the four separation lines and most of the singular points on the wall surfaces (include the upper and lower endwalls and blade surfaces) in a cascade are located in its upper half span, which leads to worse aerodynamic characteristics there.

2. The key to reduce the energy losses in turbine rotor cascade with tip clearance is to weaken the leakage flow and to reasonably distribute the two separation lines on the blade suction surface. The leakage loss, dissipation loss of the vortex energy and mixing loss can be decreased notably in these two ways.

3. The flow visualizations and the topological analyses are useful tools to get full insight into the detailed vortex structure in the cascade flow field.

REFERENCES

[1] Dallmann, U., "Topological Structure of Three-Dimensional Flow Separation," DFVLR-IB221-82 A07. Gottingen, Germany, (1983).

[2] Sears, W.R., "The Boundary Layer of Yawed Cylinders," *J. of Aerospace Sciences,* **15,** No.1, pp.49-52, (1948).

[3] Legendre, R., "Linges de Courant d'un Ecoulement Continu," La Recherche Aerospatiale, No.105, pp.3-9, (1965).

[4] Lighthill, M.J., "Attachment and Separation in Three-Dimensional Flow, Section Two 2-6, Laminar Boundary Layers," Ed. by Rosenhead, Oxford Univ. Press, pp.72-82, (1963).

[5] Hunt, J.C.R., et al., "Kinematical Studies of the Flows around Free or Surface-Mounted Obstacles; Applying Topology to Flow Visualization," *J. Fluid Mech.,* **86,** Part 1, pp. 179-200, (1978).

[6] Kang Shun, "An Application of Topological Analysis to Studying the Three-Dimensional Flow in Cascade; Part I-Topological Rules for Skin-Friction Lines and Section Streamlines," Applied Mathematics and Mechanics, **11,** No.5, pp.489-495, (English Edition), (1990).

[7] Kang Shun, et al., "An Application of Topological Analysis to Studying the Three-Dimensional Flow in Cascade; Part II-Topological Analysis on the Vector Field Pattern of Skin-Frictions and Section Streamlines," *Applied Mathematics and Mechanics,* **11,** No.5, pp.1119-1127, (English Edition), (1990).

[8] Yamamoto, A., "Endwall Flow/Loss Mechanisms in a Linear Turbine Cascade with Blade Tip Clearance," *Trans. of the ASME., J. of Turbomachinery,* **111,** pp.264-275, (1989).

[9] Sjolander, A., et al., "Effects of Tip Clearance on Blade Loading in a Planar Cascade of Turbine Blades," *Trans. of ASME., J. of Turbomachinery,* **109,** pp.237-244, (1987).